Static electric dipole polarizability of lithium atoms in Debye plasmas*

Ning Li-Na(宁丽娜)† and Qi Yue-Ying(祁月盈)

College of Mathematics, Physics and Information Engineering, Jiaxing University, Jiaxing 314001, *China*

(Received 18 June 2012; revised manuscript received 16 August 2012)

The static electric dipole polarizabilities of the ground state and $n \leq 3$ excited states of a lithium atom embedded in a weekly coupled plasma environment are investigated as a function of the plasma screening radium. The plasma screening of the Coulomb interaction is described by the Debye–Hückel potential and the interaction between the valence electron and the atomic core is described by a model potential. The electron energies and wave functions for both the bound and continuum states are calculated by solving the Schrödinger equation numerically using the symplectic integrator. The oscillator strengths, partial-wave, and total static dipole polarizabilities of the ground state and $n \leq 3$ excited states of the lithium atom are calculated. Comparison of present results with those of other authors, when available, is made. The results for the 2s ground state demonstrated that the oscillator strengths and the static dipole polarizabilities from np orbitals do not always increase or decrease with the plasma screening effect increasing, unlike that for hydrogen-like ions, especially for 2s→3p transition there is a zero value for both the oscillator strength and the static dipole polarizability for screening length $D = 10.3106a_0$, which is associated with the Cooper minima.

Keywords: static electric dipole polarizability, Debye plasmas, lithium atom

PACS: 32.10.DK, 32.80.Fb, 52.20.–j **DOI:** 10.1088/1674-1056/21/12/123201

1. Introduction

The static electric dipole polarizability (SEDP) is an important characteristic for an atomic system, which describes its response to an external electric field; and also has a significant role in collision processes involving such particles,[1,2] which is an important parameter of the long-range forces between an ion and a neutral atom; and etc. SEDP reflects the long-range dipole interaction between a charged particle and an atomic system and is related to orbital energies and orbital wave functions. A large number of studies[1,3–7] demonstrated that the plasma screening effect cannot be covered in researching the atomic structure and atomic processes in plasmas. There is a lot of experimental and theoretical information on SEDP for solated atoms, molecules, ions, and clusters.[3,8–10] SEDP of hydrogen-like atoms embedded in a plasma environment[11] and isolated alkali metal atoms[12] has been under studied, as has the oscillator strengths of the isolated lithium-like ions,[13,14] but data about SEDP for alkali metals in plasmas is very limited, especially for lithium atoms.

The screened Coulomb interaction between charged particles in hot, dense plasmas depend on plasma temperatures (T) and plasma densities (n), which divide the plasmas into inertial confinement fusion (ICF) plasmas ($n \sim 10^{22}$ cm^{-3}–10^{26} cm^{-3}, $T \sim 0.5$ keV–10 keV), laser plasmas ($n \sim 10^{19}$ cm^{-3}–10^{21} cm^{-3}, $T \sim 50$ eV–300 eV), and stellar atmospheres ($n \sim 10^{15}$ cm^{-3}–10^{18} cm^{-3}, $T \sim 0.5$ eV–5 eV). The Coulomb interaction screening in these plasmas is a collective effect of the correlated many-particle interactions, and to the lowest particle correlation order (pair-wise correlations) it reduces to the Debye–Hückel potential,[15,16]

$$V(r) = V_0(r) \exp\left(-\frac{r}{D}\right), \tag{1}$$

where $V_0(r)$ is the potential between the valence electron and the core in the free field, $D = (k_{\rm B}T_{\rm e}/4\pi e^2 n_{\rm e})^{1/2}$ is the Debye screening length, $T_{\rm e}$ and $n_{\rm e}$ are the temperature and density of the plasma electron respectively, and $k_{\rm B}$ is the Boltzmann constant. The Coulomb interaction screening in a plasma by Eq. (1) is adequate only in the condition $\Gamma \leq 1$ and $\gamma \ll 1$, where $\Gamma = e^2/(ak_{\rm B}T_{\rm e})$ is the Coulomb coupling parameter, $\gamma = e^2/(Dk_{\rm B}T_{\rm e})$ is the plasma non-ideality parameter, and $a = [3/(4\pi n_{\rm e})]^{1/3}$ is the average inter-particle distance which is related to the

*Project supported by the National Natural Science Foundation of China (Grant Nos. 11005049, 10979007, and 10974021).

†Corresponding author. E-mail: cherrynln@163.com

© 2012 Chinese Physical Society and IOP Publishing Ltd

plasma density. In spite of that, there is a wide class of laboratorial and astrophysical plasmas in which these conditions are fulfilled (or, say, Debye plasmas).

Lithium is regarded as a possible plasma-facing material in future fusion reactors. It will be emitted from the walls into the plasma. In the edge and diverter of tokomak, the plasma temperature and density are about $T_{\rm e} \sim 0.1$ eV–100 eV and $n_{\rm e} \sim 10^{12}$ cm^{-3}–10^{15} cm^{-3}, respectively, which fulfills the conditions of Debye plasmas. Thus we investigated the SEDP of the ground state 2s and $n \leq 3$ excited states for lithium atoms in Debye plasmas in our present work.

The paper is organized as follows. In the next section we briefly describe the model potential between the valence electron and the atomic core, and the theoretical method for determination of the eigenenergies and the wave functions of lithium atoms in Debye plasmas; in this section we also present the numerical method of SEDP. In Section 3 we present the results for the oscillator strengths, transition energies, partial wave, and total SEDP as functions of plasma screening parameter $1/D$. In the last section we give our conclusions. Atomic units will be used in the remaining part of this paper, unless explicitly indicated otherwise.

2. Theoretical method

In this work, the lithium atomic system is considered to be composed of two particles: the valence electron and an atomic ion core whose structure is not considered explicitly. The interaction between the valence electron and the core is described by the following model potential[17]

$$V_0(r) = -\frac{1}{r}[(Z - N_c) + N_c(\,{\rm e}^{-2\alpha r} + \beta r\,{\rm e}^{-2\gamma r})], \quad (2)$$

where $Z = 3$ and $N_{\rm c} = 2$ are the nuclear charge and the number of core electrons, and $\alpha = \beta = \gamma = 1.6559$ are chosen to optimize the orbital energies in agreement with the NIST data.[18]

With the perturbation theory framework, SEDP of an atomic system in the discrete quantum state $|n\rangle$ can be expressed in the following formula[19,20]

$$\alpha_n = 2\sum_{\kappa \neq n} \frac{|H_{n\kappa}|^2}{E_\kappa^{(0)} - E_n^{(0)}}, \quad (3)$$

where $H_{n\kappa} = \left\langle \psi_\kappa^{(0)} \right| \hat{z} \left| \psi_n^{(0)} \right\rangle$ is the dipole matrix element due to the presence of the external electric field oriented along the z direction, $\psi_n^{(0)}$, $\psi_\kappa^{(0)}$, and $E_n^{(0)}$, $E_\kappa^{(0)}$ are the wave functions and energies of states $|nlm\rangle$ and $|\kappa l'm'\rangle$ without perturbation, respectively. $\psi_\kappa^{(0)}$ in Eq. (3) denotes a discrete state or a continuum state. For the continuum state, the sum in Eq. (3) is replaced by an integral over the continuous variable $\kappa = \sqrt{2\varepsilon}$, where ε is the energy of the continuum state. For a potential with central-symmetric property, such as Eq. (2), the wave functions $\psi_n^{(0)}$ and $\psi_\kappa^{(0)}$ can be represented in the forms

$$\psi_n^{(0)} = |nlm\rangle = \frac{P_{nl}(r)}{r} {\rm Y}_{lm}(\theta, \varphi)$$

and

$$\psi_\kappa^{(0)} = |\kappa l'm'\rangle = \frac{P_{\kappa l'}(r)}{r} {\rm Y}_{l'm'}(\theta, \varphi)$$

l and l' are the angular quantum numbers, m and m' are the magnetic quantum numbers, respectively, and thus SEDP of the atom in the state $|nlm\rangle$

$$\begin{aligned}\alpha_{nlm} &= 2\sum_{\kappa l'm' \neq nlm} \frac{\langle \kappa l'm' |\, \hat{z}\, | nlm\rangle}{E_{\kappa l'} - E_{nl}} \\ &= 2\sum_{\kappa l'm' \neq nlm} \frac{\left(M_{nl}^{\kappa l'}\right)^2}{E_{\kappa l'} - E_{nl}} (2l+1)(2l'+1) \\ &\quad \times \begin{pmatrix} l & 1 & l' \\ 0 & 0 & 0 \end{pmatrix}^2 \begin{pmatrix} l' & 1 & l \\ -m' & 0 & m \end{pmatrix}^2, \end{aligned} \quad (4)$$

here $M_{nl,\kappa l'} = \int_0^\infty P_{\kappa l'}(r)\, r P_{nl}(r)\, {\rm d}r$ is the dipole matrix element, and $\begin{pmatrix} a & b & c \\ d & e & f \end{pmatrix}$ is a Wigner $3-j$ symbol.[19,21,22] Thus the calculation of SEDP of a lithium atom in the state $|nlm\rangle$ in a Debye plasma is reduced to solve the radial Schrödinger equation with the potentials Eqs. (1) and (2) in both the discrete and continuous spectra.

In the non-relativistic approximation, the radial Schrödinger equation for a lithium atom in a Debye plasma is given by

$$\left(-\frac{1}{2}\frac{{\rm d}^2}{{\rm d}r^2} + \frac{l(l+1)}{2r^2} + V(r)\right) P_{\kappa l}(r) = E_{\kappa l} P_{\kappa l}(r). \quad (5)$$

Equation (5) has been subject to solution in the past by a variety of methods, such as perturbation approximate,[23] variational,[24] and direct numerical integration methods.[4] In the present work we solve Eq. (5) by employing the symplectic integration scheme described in Refs. [25]–[27] in detail. The radial wave functions of discrete states are orthogonal-normalized in the conventional way and that of continuum states are normalized to a unit energy interval,

respectively, as follows:

$$\int_0^\infty \mathrm{d}r P_{nl}(r) P_{n'l'}(r) = \delta_{n,n'}\delta_{l,l'}, \quad (6)$$

$$\int_0^\infty \mathrm{d}r P_{El}(r) \int_{E-\Delta E}^{E+\Delta E} P_{E'l}(r)\mathrm{d}E' = \delta_{l,l'}. \quad (7)$$

3. Results and discussion

As it is well known,[19] there is only a finite number of bound states due to the potential with Eq. (1) for any finite value of Debye screening length D. With increasing the screening effect (decreasing the value of D), the binding energy of a given discrete state decreases and at a certain critical value of D, it merges into the continuum edge. The values of the critical screening lengths D^{c}_{nl} for a lithium atom are shown in Table 1. That is to say, the discrete state $|nl\rangle$ merges into the continuum when screening length $D < D^{\mathrm{c}}_{nl}$. Therefore, with decreasing D, the number of bound states decreases, and thus reduces the number of the sum terms in Eq. (4) over the discrete spectrum. It is in contrast with the unscreened case where the sum in Eq. (4) over the discrete spectrum includes an infinite number of terms.

Table 1. Values of the critical screening lengths D^{c}_{nl} for lithium atom in units of a_0.

n	l		
	s	p	d
2	2.11526	4.45625	
3	5.42024	8.69809	10.9461
4	10.2972	14.4715	17.2071

We list the orbital energies $E_{2\mathrm{s}}$, transition energies $\Delta E_{2\mathrm{s},n\mathrm{p}} = E^{(0)}_{n\mathrm{p}} - E^{(0)}_{2\mathrm{s}}$, absorption oscillator strengths $f_{2\mathrm{s},n\mathrm{p}}$, and dipole matrix elements $M_{2\mathrm{s},n\mathrm{p}}$ ($n \leq 4$) with different screening lengths in Table 2. It is obvious that the smaller the screening length is, the smaller the transition energy is. We also compare the transition energies and oscillator strengths for 2s→ np transitions without screening obtained in the present work and in Ref. [18] in Table 2. The transition energies agree quite well, and meanwhile, the differences in the oscillator strengths are a little significant. The differences in the oscillator strengths are caused by using different potentials in calculations. These differences will not influence the results, for what we focus on is the plasma screening effect.

Table 2. Ground-state energies, transition energies, oscillator strengths, and dipole matrix elements of a lithium atom for various screening lengths D, a.u.: atomic unit.

D/a_0	$E_{2\mathrm{s}}$/a.u.	Transition process	Transition energy/a.u.	Oscillator strength $f_{2\mathrm{s},n\mathrm{p}}$	Dipole matrix element $M_{2\mathrm{s},n\mathrm{p}}$
∞	–0.1981	2s→2p	0.06821 (0.06791)[18]	0.75269 (0.74696)[18]	–4.06854
		2s→3p	0.14094 (0.14091)[18]	0.00415 (0.00471)[18]	0.21027
		2s→4p	0.16617 (0.16617)[18]	0.00396 (0.00421)[18]	0.18913
50	–0.1785	2s→2p	0.06775	0.75383	–4.08539
		2s→3p	0.13908	0.00369	0.19937
		2s→4p	0.16262	0.00332	0.17487
33	–0.1689	2s→2p	0.06739	0.75538	–4.10044
		2s→3p	0.13713	0.00311	0.18454
		2s→4p	0.15880	0.00263	0.15767
15	–0.1379	2s→2p	0.06555	0.76512	–4.18434
		2s→3p	0.12599	0.00069	0.09086
		2s→4p	0.13778	0.00022	0.04921
11	–0.1195	2s→2p	0.06385	0.77433	–4.26515
		2s→3p	0.11554	1.5×10^{-9}	0.00014
10	–0.1131	2s→2p	0.06311	0.77810	–4.30036
		2s→3p	0.11107	0.00009	–0.03530
9.0	–0.1055	2s→2p	0.06214	0.78278	–4.34692
		2s→3p	0.10515	0.00034	–0.06963
5.0	–0.0560	2s→2p	0.05070	0.76307	–4.75164
4.8	–0.0523	2s→2p	0.04914	0.73384	–4.73284
4.5	–0.0465	2s→2p	0.04617	0.59981	–4.41434

Oscillator strength as a function of the screening parameter $1/D$ is shown in Fig. 1. It displays that the oscillator strength for 2s→2p transition increases first and then decreases when decreasing D and has a maximum value at $D = 6.0a_0$ and that for 2s→3p transition decreases first and then increases and has obviously a zero value at a special screening length $D = 10.3106a_0$, and that for 2s→4p monotonously decreases. These behaviors of oscillator strengths result from the behavior of the dipole matrix elements, which are also listed in Table 2. Anyhow, the oscillator strength for $n \neq n'$ does not always increase or decrease with the screening length, not like that for hydrogen-like ions,[11] which decreases with reducing the screening length.

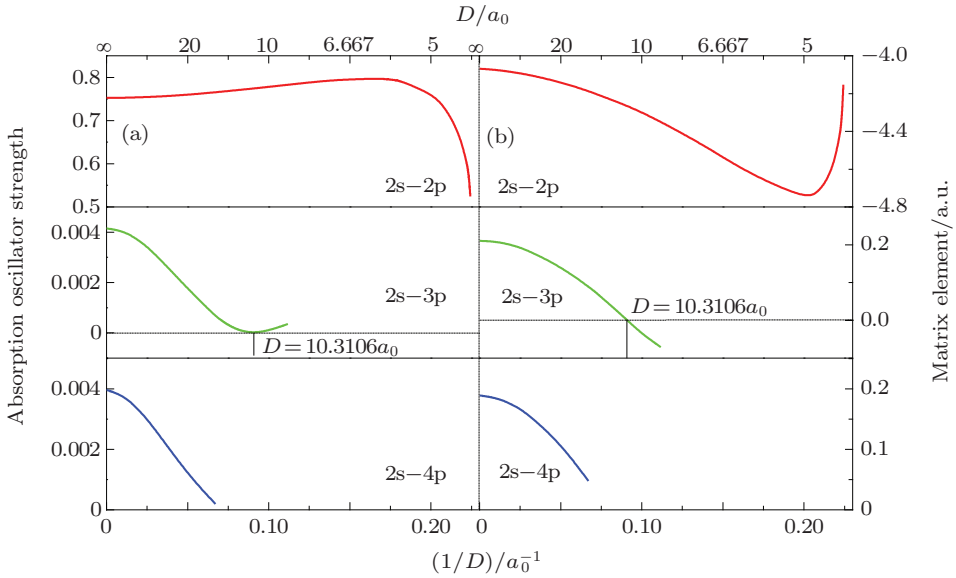


Fig. 1. (color online) The absorption oscillator strengths $f_{2s,np}$ and matrix elements $M_{2s,np}$ ($n \leq 4$) as a function of the screening parameter $1/D$.

Table 3. Static electric dipole polarizabilities α_{2s} of the ground-state 2s for lithium atom for a number of screening lengths D.

D/a_0	Polarizability	Continuum state	Bound states	Major contributions for bound states		
				2p	3p	4p
∞	163.737 164.084[28] 164.0(3.4)[8]	1.24004	162.497	161.790	0.20915	0.14350
100	164.575	1.32855	163.247	162.742	0.20555	0.13901
50	166.061	1.41459	164.646	164.241	0.19053	0.12537
33	168.140	1.49386	166.646	166.331	0.16556	0.10436
20	173.603	1.61296	171.990	171.836	0.10091	0.05312
15	179.788	1.65965	178.128	178.073	0.04368	0.01172
11	191.577	1.63174	189.945	189.945	1.2E-07	
10	196.956	1.60334	195.352	195.345	0.00748	
9	204.328	1.57233	202.756	202.725	0.03074	
8	214.935	1.66277	213.272	213.272		
7	231.222	1.97915	229.243	229.243		
6	258.788	3.58745	255.201	255.201		
5	313.434	16.5219	296.912	296.912		
4.8	331.174	27.2954	303.878	303.878		
4.5	365.698	84.3345	281.364	281.364		
4.0	483.808	483.808	–			
3.6	611.797	611.797	–			
3	1394.09	1394.09	–			
2.8	2354.20	2354.20	–			
2.5	10126.6	10126.6	–			
2.4	24875.2	24875.2	–			
2.3	102554	102554	–			
2.2	1678363	1678363	–			

In Table 3, we show the dipole polarizabilities of the ground state 2s for lithium atom for a number of screening lengths. The total contributions of the continuum states, partial-wave contribution of bound states 2p, 3p, and 4p to SEDP and the datum of α_{2s} without screening from Refs. [8] and [28] are tabulated in this table. It can be seen that our results are in excellent agreement with the measured data within experimental errors and is in harmony with other theoretical data. This demonstrates that our calculations are reliable and accurate. For the case without screening, a small difference between our data and the experimental data is caused by the sum in Eq. (4) over the discrete spectrum, because the infinite summation in Eq. (4) is replaced by a finite case, and we just considered the summation about the $n \leq 20$ states, which minimized the total dipole polarizability without screening. It should be noted that the contribution from the bound states is always dominant until the first excited state 2p disappears ($D < D^{c}_{2p} = 4.45625a_0$). After all of the bound p orbitals disappear, the contribution from the continuum state increases dramatically.

We noticed that the behaviors in the oscillator strength will appear in SEDP, because the relation between the oscillator strength and the static polarizability can be expressed as[20]

$$\alpha_{nlm} = 3(2l+1) \sum_{\kappa l' m' \neq nlm} \frac{f_{nl,kl'}}{(E_{\kappa l'} - E_{nl})^2} \times \begin{pmatrix} l' & 1 & l \\ -m' & 0 & m \end{pmatrix}^2 . \quad (8)$$

From Table 3 it can be seen that, with decreasing D, the contribution from 2p orbital for SEDP increases and then decreases, and that from 3p orbital decreases and then increases, and that from the 4p orbital keeps decreasing, but it does not influence the total dipole polarizability, which increases dramatically with decreasing D. This behavior of SEDP is similar to that of the oscillator strength; only the position of the screening length at which SEDP gets to the maximum value is different from that at which the oscillator strength gets to the maximum value. For the transition 2s→2p, the energy difference monotonously decreases, but the square of the matrix element ($M_{2s,2p} < 0$) increases and then decreases with decreasing D, and so there are different positions of the maximum value for SEDP and oscillator strength. For the transition 2s→3p, the position of the zero value for SEDP is the same as that for the oscillator strength; they are both proportional to the square of the matrix element. When the matrix element changes from positive to negative, the zero will exist in SEDP and the oscillator strength, and also the photo-ionization cross section, which is the Cooper minima.[29,30]

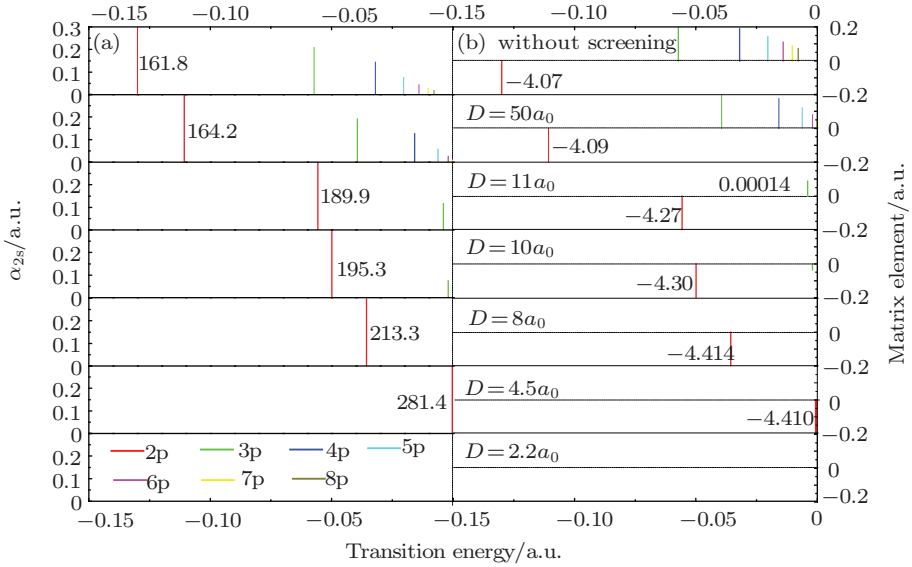


Fig. 2. (color online) (a) Contributions to α_{2s} from individual bound states for a lithium atom for unscreened and screened cases with a number of screening lengths. The numbers beside the lines are the actual values of the partial polarizability from 2p states. (b) Dipole matrix elements $M_{2s,np}$. The numbers beside the red lines are the actual values of the dipole matrix elements between 2s→2p. The matrix element between 2s→3p changes from positive to negative between $D = 11a_0$ and $D = 10a_0$.

The differential contributions for SEDP from the individual bound states and the continuum for a number of screening lengths are shown in Fig. 2(a) and Fig. 3(a). The heights of the vertical lines in Fig. 2(a) correspond to the values of α_{2s} in Table 3 for a given state and a given screening length D. From this figure, it is obvious that with decreasing D, the number of bound states np contributing to α_{2s} is less and less when np orbitals successively enters into the continuum. When $D = 8.0a_0$, only 2p orbital still stay in the discrete spectrum, but when $D < D^c_{2p} = 4.45625a_0$, α_{2s} all originates from the polarization to continuum states. In Fig. 3(a), there is a minimum in the curve of polarizability as a function of continuum state energy for some given D, which is equal to zero. The position of the zero value is different for different plasma screening lengths D, only existing for $D < 10.3106a_0$ (seen from Fig. 4), associated with the zero value of the matrix element for 2s→ εp, as shown in Fig. 3(b), and is the so-called Cooper minima. It can be obviously seen in Figs. 3(a) and 3(b) that the Cooper minima move to higher continuum energy ε^c with deceasing D. When ε^c gets across zero, the Cooper minima disappear and merge into the bound–bound transitions. This screening length is $D = 10.3106a_0$, where the matrix element for 2s→3p changes from positive to negative (Fig. 2(b) and Fig. 1(b)). When $D > 10.3106a_0$, this zero value is covered in the transition 2s→3p (seen from Table 2). Figure 4 shows the energy position ε^c of the Cooper minima as a function of the screening length D.

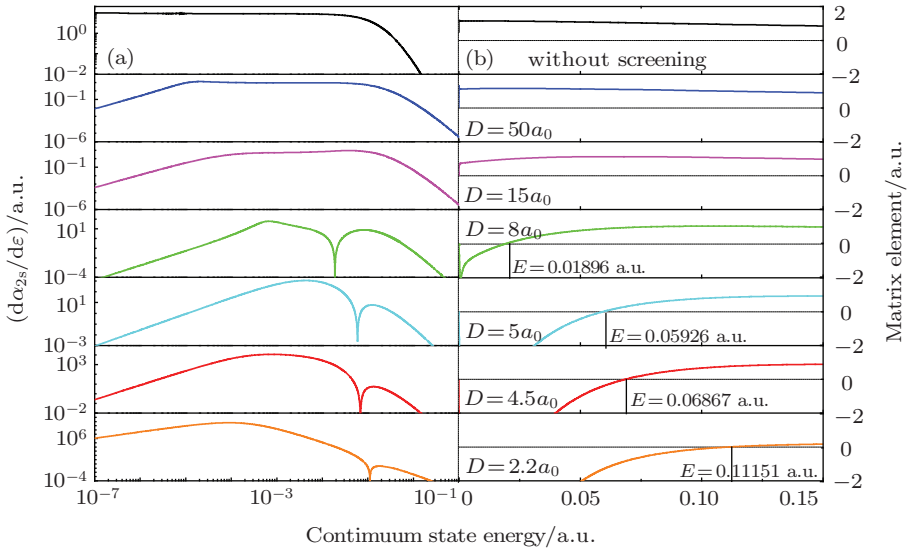


Fig. 3. (color online) (a) Contributions to α_{2s} from continuum states for a lithium atom for unscreened and screened cases with a number of screening lengths. (Note the scale change for $d\alpha/d\varepsilon$, and the logarithmic scale for both the horizontal and longitudinal coordinates.) (b) Dipole matrix elements $M_{2s,\varepsilon p}$. The Cooper minima in panel (a) correspond to the zero points of the matrix elements, marked in panel (b).

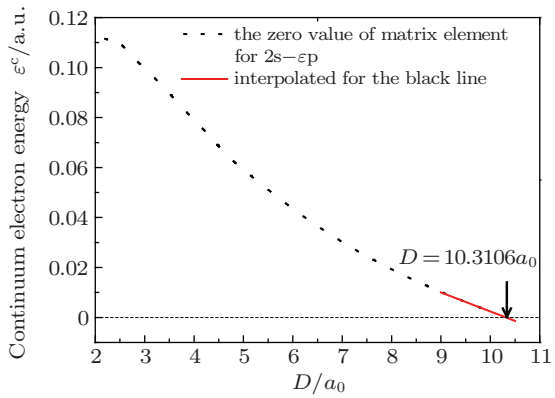


Fig. 4. (color online) The relationship between the Cooper minima position ε^c and the screening lengths D.

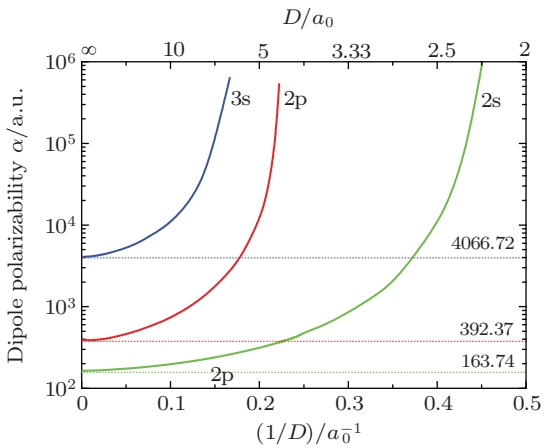


Fig. 5. (color online) The dipole polarizabilities of 2s, 2p, and 3s states for a lithium atom as functions of screening parameter $1/D$. The limiting $D \to \infty$ value of 163.74 a.u., 292.37 a.u., and 4066.72 a.u. for 2s, 2p, and 3s respectively is the polarizability in the pure Coulomb case.

Now we observe the results of the total polarizabilities. SEDP for 2s, 2p, and 3s orbitals as functions of screening parameter $1/D$ are shown in Fig. 5. SEDPs dramatically increase with increasing plasma effect, especially, when D is close to its critical screening length $D^{\rm c}_{nl}$, the polarizability reaches the magnitudes of 10^6, but we know that it has lost its physical meaning because the electron is already in the continuum state. The dramatic increase in the polarizability when $D \to D^{\rm c}_{nl}$ is a mere result of a strong overlap of bound-state wave function with the continuum wave function in the strong coupled plasmas. In contrast, the calculated polarizability in the limit $D \to \infty$ (without screening) is in agreement with the experiment datum and other theoretical values.[8,28]

4. Conclusions

In summary, we have investigated the static dipole polarizabilities $\alpha_{2\rm s}$, $\alpha_{2\rm p}$, and $\alpha_{3\rm s}$ of a lithium atom embedded in Debye plasmas. The results demonstrated that SEDP dramatically increases with increasing plasma effect, just like it does for hydrogen-like ions.[11] The behaviors of the oscillator strength and partial-wave contribution to SEDP for 2s$\to$ np transitions are nearly the same: for 2s$\to$2p transition, they increases first and then decreases with decreasing D, but the position of the screening length at which they get to the maximum value is different ($D = 6.0a_0$ for oscillator strength and $D = 4.8a_0$ for SEDP); for 2s$\to$3p transition, they decreases first and then increase and obviously have a zero value at a special screening length $D = 10.3106a_0$, at which the matrix element changes from positive to negative, for both the oscillator strength and SEDP; for 2s$\to$4p transition, they keeps decreasing. The behaviors of the oscillator strength for 2s$\to$ np transitions of lithium atom mentioned above are different from that of the hydrogen-like ions: they do not always increase or decrease with the screening length, whatever $n = 2$ or $n \neq 2$ for lithium atom; they decrease for $n \neq 2$ and increase for $n = 2$ with reducing the screening length for hydrogen-like ions.[26] But the total SEDP for the considered orbital of lithium atom has the same behavior as those of hydrogen-like ions: they monotonously increase with the plasma screening effect increasing (the plasma screening length decreases).

In addition, the Cooper minima appear in the transition 2s$\to$ εp, and shift to the higher energy when the plasma screening effect increases, and are covered in the bound–bound transition for $D > 10.3106a_0$ and unscreened cases. The results reported here should be useful in the interpretation of the spectral properties of lithium atoms in laboratorial and astrophysical Debye plasmas.

References

[1] Miller T M and Bederson B 1978 *Adv. At. Mol. Phys.* **13** 1

[2] Chu X, Dalgarno A and Groenenboom G C 2007 *Phys. Rev.* A **75** 032723

[3] Miller T M 1995 *Atomic and Molecular Polarizability* Vol. 75 (Boca Raton FL: CRC Press)

[4] Rogers F J, Graboske H C and Harwood D J 1970 *Phys. Rev.* A **1** 1577

[5] Ding Q Y, Zhang S B and Wang J G 2011 *Chin. Phys. Lett.* **28** 053202

[6] Zhang S B, Qi Y Y, Qü Y Z, Chen X J and Wang J G 2010 *Chin. Phys. Lett.* **27** 013401

[7] Zhao J M, Zhang L J, Feng Z G, Li C Y and Jia S T 2010 *Chin. Phys.* B **19** 043202

[8] Molof R W, Schwartz H L, Miller T M and Bederson B 1974 *Phys. Rev.* A **10** 1131

[9] Tang L Y, Zhang Y H, Zhang X Z, Jiang J and Mitroy J 2012 *Phys. Rev.* A **86** 012505

[10] Li X B, Wang H Y, Luo J S, Guo Y D, Wu W D and Tang Y J 2009 *Chin. Phys.* B **18** 3414

[11] Qi Y Y, Wang J G and Janev R K 2009 *Phys. Rev.* A **80** 032502

[12] Tang L Y, Yan Z C, Shi T Y and James F Babb 2009 *Phys. Rev.* A **79** 062712

[13] Hu M H and Wang Z W 2004 *Chin. Phys.* **13** 1246

[14] Hu M H and Wang Z W 2009 *Chin. Phys.* B **18** 2244

[15] Salzman D 1998 *Atomic Physics in Hot Plasmas* (New York: Ocford University Press) pp. 16–56

[16] Murillo M S and Weisheit J C 1998 *Phys. Rep.* **302** 1

[17] Saboo S and Ho Y K 2006 *Phys. Plasmas* **13** 063301

[18] NIST data; see website www.physics.nist.gov, 2008

[19] Landau L D and Lifshitz E M 1958 *Quantum Mechanics: Nonrelativistic Theory* (London: Pergamon)

[20] Dalgarno A and Lynn N 1957 *Proc. Roy. Soc.* A **70** 223

[21] Cowan R W 1981 *The Theory of Atomic Structure and Spectra* (Berkeley: University of California Press)

[22] Fang Q Y and Yan J 2006 *The Theory of Atomic Structure, Collisions and Spectra* (Beijing: National Defence Industry Press) pp. 36–40 (in Chinese)

[23] Chandhury P and Bhattacharyya S P 1998 *Chem. Phys. Lett.* **296** 51

[24] Stubbins C 1993 *Phys. Rev.* A **48** 220

[25] Forest E and Ruth R D 1990 *Physica* D **43** 105

[26] Qi Y Y, Wang J G and Janev R K 2008 *Phys. Rev.* A **78** 062511

[27] Qi Y Y, Wu Y, Wang J G and Ding P Z 2008 *Chin. Phys. Lett.* **25** 3620

[28] Johnson W R, Safronova U I, Derevianko A and Safronova M S 2008 *Phys. Rev.* A **77** 022510-1-9

[29] Qi Y Y, Wu Y and Wang J G 2009 *Phys. Plasmas* **16** 033507

[30] Qi Y Y, Wang J G and Janev R K 2011 *Eur. Phys. J.* D **63** 327